0026-895X/07/7206-1576–1585$20.00
MOLECULAR PHARMACOLOGY
Copyright © 2007 The American Society for Pharmacology and Experimental Therapeutics
Mol Pharmacol 72:1576–1585, 2007

Vol. 72, No. 6
37150/3274474
Printed in U.S.A.

Inhibition of TRPP3 Channel by Amiloride and Analogs

Xiao-Qing Dai, Alkarim Ramji, Yan Liu, Qiang Li, Edward Karpinski, and Xing-Zhen Chen

Membrane Protein Research Group, Department of Physiology, University of Alberta, Edmonton, Alberta, Canada

Received April 16, 2007; accepted September 4, 2007

ABSTRACT

TRPP3, a member of the transient receptor potential (TRP) superfamily of cation channels, is a Ca^{2+}-activated channel permeable to Ca^{2+}, Na^{+}, and K^{+}. TRPP3 has been implicated in sour tasting in bipolar cells of tongue and in regulation of pH-sensitive action potential in spinal cord neurons. TRPP3 is also present in excitable and nonexcitable cells of other tissues, including retina, brain, heart, testis, and kidney, with unknown functions. In this study, we examined the functional modulation of TRPP3 channel by amiloride and its analogs, known to inhibit several ion channels and transporters and respond to all taste stimuli, using *Xenopus laevis* oocyte expression, electrophysiology, and radiotracer measurements. We found that amiloride and its analogs inhibit TRPP3 channel activities with different affinities. Radiolabeled $^{45}Ca^{2+}$ uptake showed that TRPP3-mediated Ca^{2+} transport was inhibited by amiloride, phenamil, benzamil, and 5-(*N*-ethyl-*N*-isopropyl)amiloride (EIPA). Two-microelectrode voltage clamp experiments revealed that TRPP3-mediated Ca^{2+}-activated currents are substantially inhibited by amiloride analogs, in an order of potency of phenamil > benzamil > EIPA > amiloride, with IC_{50} values of 0.14, 1.1, 10.5, and 143 μM, respectively. The inhibition potency positively correlated with the size of inhibitors. Using cell-attached patch clamping, we showed that the amiloride analogs decrease the open probability and mean open time but have no effect on single-channel conductance. Study of inhibition by phenamil in the presence of previously reported inhibitor tetrapentylammonium indicates that amiloride and organic cation inhibitors compete for binding the same site on TRPP3. TRPP3 may contribute to previously reported in vivo amiloride-sensitive cation transport.

TRPP3 (also called polycystin-L), initially cloned from human retina expressed sequence tag (Nomura et al., 1998; Wu et al., 1998), is a novel member of the transient receptor potential (TRP) superfamily of cation channels. TRPP3 has two homologs, TRPP2 (or polycystin-2) and TRPP5 (or polycystin-2L2), which share amino acid sequence similarity of ~70%. TRPP2 is part of a flow sensor, and its mutations account for ~10% of autosomal dominant polycystic kidney disease (ADPKD), whereas the function and physiological roles of TRPP5 remain unknown. TRPP3 is localized to a subset of taste receptor cells in the tongue, where it may play a crucial role in sour tasting (Huang et al., 2006; Ishimaru et al., 2006; LopezJimenez et al., 2006), and to neurons surrounding the central canal of the spinal cord, where it may account for the long-sought proton-dependent regulation of the frequency of action potential (Huang et al., 2006). TRPP3 is present in neuronal or non-neuronal (e.g., epithelial) cells of other tissues, such as kidney, heart, retina, testis, liver, pancreas, and spleen (Basora et al., 2002). In fact, TRPP3 is found in the ganglion cells of retina and collecting duct epithelial cells of kidney. However, the function of TRPP3 in retina has not been reported. It is thus interesting to determine whether there exists a common mechanism underlying its physiological roles in various tissues.

TRPP3 is a Ca^{2+}-activated nonselective cation channel permeable to Ca^{2+}, K^{+}, Na^{+}, Rb^{+}, NH_4, and Ba^{2+}, inhibited by Mg^{2+}, H^{+}, La^{3+}, and Gd^{3+} (Chen et al., 1999; Liu et al., 2002). Based on its permeability to monovalent organic cations (methlyamine, dimethylamine, triethylamine, and tetramethylammonium) and inhibition by larger compounds [tetraethylammonium, tetrapropylammonium, tetrabutylammonium and tetrapentylammonium (TPeA)], a pore size of ~7 Å was estimated (Dai et al., 2006). TRPP3 is not a voltage-gated channel, but its channel properties show significant voltage dependence (Chen et al., 1999; Liu et al., 2002). It is noteworthy that coexpression of TRPP3 with polycystin-1, a large receptor-like membrane protein mutated in 80 to 85% of ADPKD, in human embryonic kidney

This work was supported by the Canadian Institutes of Health Research, the Alberta Heritage Foundation for Medical Research (AHFMR), and the Kidney Foundation of Canada (to X.-Z.C.). X.-Z.C. is an AHFMR Senior Scholar. X.-Q.D. is the recipient of an AHFMR Studentship.

Article, publication date, and citation information can be found at http://molpharm.aspetjournals.org.

doi:10.1124/mol.107.037150.

ABBREVIATIONS: TRP, transient receptor potential; ADPKD, autosomal dominant polycystic kidney disease; ARPKD, autosomal recessive polycystic kidney disease; EIPA, 5-(*N*-ethyl-*N*-isopropyl) amiloride; ENaC, epithelial sodium channel; MOT, mean open time; NP_o, open probability; ANOVA, analysis of variance; TPeA, tetrapentylammonium; I-V, current-voltage relationships; TRPP2: transient receptor potential polycystin-2; TRPP3: transient receptor potential polycystin-L; TRPP5: transient receptor potential polycystin-2L2.

293 cells resulted in TRPP3 trafficking to the plasma membrane, where TRPP3 seemed to mediate Ca^{2+} entry in the presence of a hypo-osmotic extracellular solution (Murakami et al., 2005). Coexpression of mouse TRPP3 and polycystin-1L3, an isoform of polycystin-1 with unknown function, but not the expression of TRPP3 or polycystin-1L3 alone, also target to the plasma membrane of human embryonic kidney 293 cells and mediate pH-activated cation conductance (Ishimaru et al., 2006). Whether the presence of polycystin-1L3, cell type and/or species difference account for the observed opposite pH dependence of TRPP3 function remain to be elucidated (Chen et al., 1999; Ishimaru et al., 2006). On the other hand, TRPP2 is a Ca^{2+}-permeable nonselective cation channel involved in ER Ca^{2+} homeostasis (González-Perrett et al., 2001; Koulen et al., 2002) and, together with polycystin-1, forms a channel complex that acts as part of flow sensor in renal epithelial primary cilia (Nauli et al., 2003). Thus, like other TRP members, TRPP2 and TRPP3 are likely to be part of cellular sensors (Clapham, 2003).

Amiloride (or *N*-amidino-3,5-diamino-6-chloropyrazinecarboxamide) and its analogs, such as 5-(*N*-ethyl-*N*-isopropyl) amiloride (EIPA), benzamil, and phenamil (Fig. 1A), have been extensively used as probes for a wide variety of transport systems (Kleyman and Cragoe, 1988). Amiloride is a well known antagonist of ENaC, Na^+/Ca^{2+}, and Na^+/H^+ exchangers, nonselective cation channels, and voltage-gated K^+ and Ca^{2+} channels (Kleyman and Cragoe, 1988, 1990; Sariban-Sohraby and Benos, 1986; Tytgat et al., 1990; Doi and Marunaka, 1995; Murata et al., 1995; Stoner and Viggiano, 2000; Hirsh, 2002). It is noteworthy that amiloride has been reported to inhibit all types of taste responses (sweet, bitter, umami, salty, and sour) (Gilbertson et al., 1993; Lilley et al., 2004). In this study, we examined the inhibitory effects of amiloride analogs on TRPP3, using *Xenopus laevis* oocyte expression in combination with whole-cell and single-channel electrophysiology, as well as radiotracer uptake measurements.

Materials and Methods

Oocyte preparation. Capped synthetic human TRPP3 mRNA was synthesized by in vitro transcription from a linearized template, using the mMessage mMachine 1 Kit (Ambion, Austin, TX). Stage V to VI oocytes were extracted from *X. laevis* and defolliculated by collagenase type I (2.5 mg/ml) (Sigma-Aldrich Canada, Oakville, ON, Canada) in the Barth's solution (88 mM NaCl, 1 mM KCl, 0.33 mM $Ca(NO_3)_2$, 0.41 mM $CaCl_2$, 0.82 mM $MgSO_4$, 2.4 mM $NaHCO_3$, and 10 mM HEPES, pH 7.5) at room temperature for approximately 2 h. Each oocyte was injected with 50 nl of RNase-free water containing 25 ng of TRPP3 mRNA 5 to 20 h after defolliculation. An equal volume of RNase-free water was injected into each control oocyte. Injected oocytes were incubated at 18°C in the Barth's solution supplemented with antibiotics (penicillin-streptomycin; Invitrogen Corporation, Carlsbad, CA) for 2 to 4 days before experiments. The animal experimentation was performed in accordance with the University of Alberta regulation concerning animal welfare.

$^{45}Ca^{2+}$ Uptake Measurement. Radiotracer uptake experiments were performed as described previously (Chen et al., 1999). In brief, the uptake solution was composed of the NaCl-containing solution (100 mM NaCl, 2 mM KCl, 1 mM $MgCl_2$, and 10 mM HEPES, pH 7.5) plus 1 mM nonradiolabeled $CaCl_2$ and 1:1000 radiolabeled $^{45}Ca^{2+}$ with a specific activity of 2 μCi/μl (GE Healthcare, Montreal, QC, Canada). Ten oocytes were incubated in 0.5 ml of the uptake solution, for 30 min with gentle shaking from time to time. Uptake was terminated by washing oocytes in the ice-cold NaCl-containing solution. Amiloride, EIPA, benzamil, and phenamil were purchased from Sigma-Aldrich Canada.

Two-Microelectrode Voltage Clamp. Two-microelectrode voltage clamp was performed as described previously (Liu et al., 2002; Dai et al., 2006). In brief, the two electrodes (capillary pipettes; Warner Instruments, Hamden, CT) impaling *X. laevis* oocytes were filled with 3 M KCl to form a tip resistance of 0.3~3 MΩ. Oocyte voltages and whole-cell currents were recorded using an amplifier (Geneclamp 500B; Molecular Devices, Sunnyvale, CA) and pClamp 9 software (Molecular Devices), and stored in a PC computer after analog-to-digital conversion (Digidata 1320A; Molecular Devices). Currents and voltages were sampled at intervals of 200 μs and filtered at 2 kHz using an eight-pole Bessel filter. In experiments using a "gap-free" (continuous acquisition at a holding voltage) or ramp protocol (Fig. 2B, top), current/voltage signals were sampled at intervals of 0.2 or 200 ms, respectively. Standard NaCl-containing solution contained: 100 mM NaCl, 2 mM KCl, 0.2 mM $MgCl_2$, and 10 mM HEPES, pH 7.5.

Patch Clamp. The vitelline layer of oocytes was manually removed after incubation at room temperature in a hypertonic solution (Barth's solution plus 200 mM sucrose). Oocytes were then transferred to a recording chamber with Barth's solution and allowed to recover for 10~20 min before clamping. Electrodes were filled with a

A

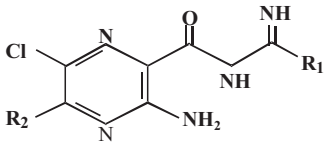

	AM	Benzamil	EIPA	Phenamil
R_1	$-NH_2$	-NH 	$-NH_2$	-NH 
R_2	$-NH_2$	$-NH_2$	-N(CH3)CH3 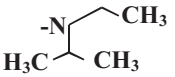	$-NH_2$

B

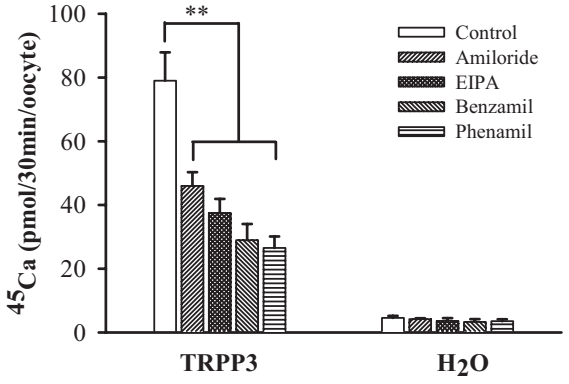

Fig. 1. Effects of amiloride analogs on the uptake mediated by TRPP3 expressed in *X. laevis* oocytes. A, chemical structures of amiloride and its analogs [from CHEMnetBASE(http://www.chemnetbase.com) for amiloride, EIPA, and benzamil; from Sigma-Aldrich (http://www.sigmaaldrich.com) for phenamil]. B, uptake of radioactive $^{45}Ca^{2+}$ mediated by TRPP3 channel using the standard NaCl-containing solution, plus 1 mM nonradiolabeled $CaCl_2$ and radiolabeled $^{45}Ca^{2+}$ in the presence and absence of 500 μM amiloride, 10 μM phenamil, 10 μM benzamil, or 100 μM EIPA. Data shown are averages from six independent measurements. Control uptake level was obtained using H_2O-injected oocytes. ** indicates very significant inhibition: $P < 0.01$.

pipette solution containing 123 mM K^+ (110 mM KCl, 13 mM KOH, and 10 mM HEPES, pH 7.4) to form tip resistance of 3–8 MΩ. Single-channel currents were recorded in cell-attached configuration using 3900A Patch Clamp amplifier (Dagan Corp., Minneapolis, MN), DigiData 1322A interface, and pClamp 9 software. Recording started after seal resistance reached at least 3 GΩ. Current and voltage signals were sampled every 200 μs and filtered at 2 kHz.

Statistics and Data Analysis. Data obtained from the two-microelectrode voltage-clamp and patch-clamp experiments were analyzed using Clampfit 9. For single-channel event detection, automatic level update was used (with 10% contribution), and the threshold value was equal to 50% of the current amplitude. Single-channel conductance values were obtained from Gaussian fits to density plots (all-point histograms). The open probability times the number of channels in the patch (NP_o, designated "open probability" hereafter) and channel mean open time (MOT) values were obtained from currents generated either by voltage pulses of 10 s per pulse or by 10-s gap-free recordings For the MOT analysis, recordings with single openings were used without filtering. Analyzed data were plotted using SigmaPlot 9 (Systat Software, Point Richmond, CA) and expressed in the form of mean ± S.E.M. (n), where n indicates the number of oocytes (or oocyte patches) tested. Data filtering and curve fitting were performed using Clampfit 9 and SigmaPlot 9, respectively. The diameters of amiloride and its analogs were measured with Spartan 4 (Wavefunction Inc., Irvine, CA). Concentration-dependent curves were fitted with the following three-parameter logistic equation: $I/I_{max} = 1/[1 + ([B]/IC_{50})^{n_H}]$, where [B] represents the concentration of amiloride or its analog, and n_H represents the Hill coefficient. Comparisons between two sets of data were analyzed by t test or two-way ANOVA, and a probability value (P) of less than 0.05 or 0.01 was considered significant or very significant, respectively.

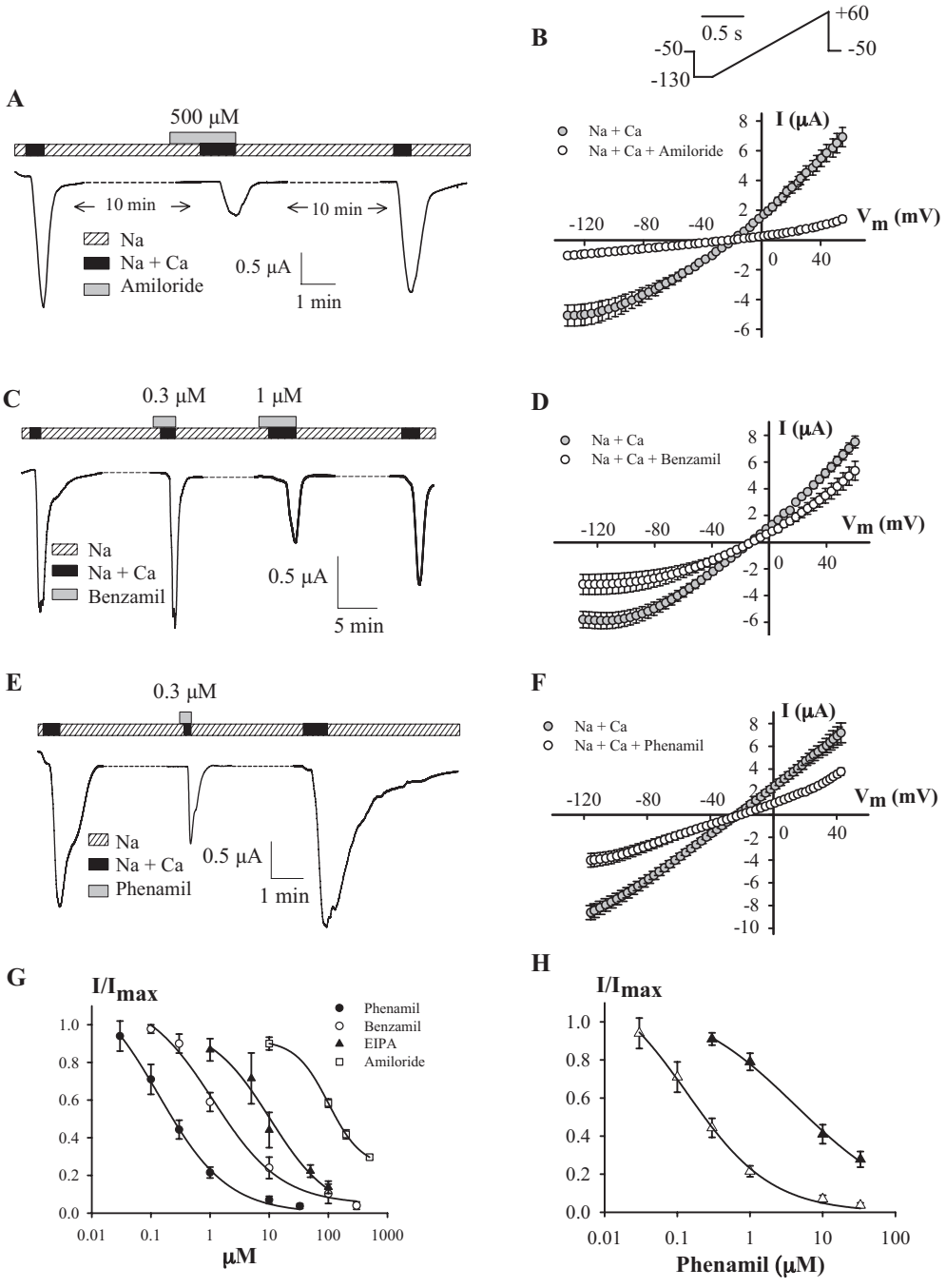

Fig. 2. Effects of amiloride analogs on the Ca^{2+}-activated whole-cell currents mediated by TRPP3 channel. A, the TRPP3-mediated whole-cell currents obtained using the two-microelectrode voltage clamp. Currents carried by Na^+ and Ca^{2+} were measured at −50 mV in the presence of the standard NaCl-containing solution ("Na") ± Ca^{2+} (5 mM) ± amiloride (500 μM). The duration between consecutive applications of 5 mM Ca^{2+} was 10 min, for the TRPP3 channels to recover (same in C and E). "Na + Ca" = the NaCl-containing solution + 5 mM $CaCl_2$. "Amiloride" = 500 μM amiloride. B, averaged current-voltage relationships (I-V curves) in the presence or absence of 500 μM amiloride (n = 16), obtained using a voltage ramp protocol (top). C, effects of benzamil on the TRPP3-mediated whole-cell currents under voltage clamp (−50 mV). D, averaged I-V curves in the presence or absence of 1 μM benzamil (n = 15). E, effects of 0.3 μM phenamil on the whole-cell currents at −50 mV. F, averaged I-V curves in the presence or absence of 0.3 μM phenamil (n = 13). G, averaged concentration-dependent curves for amiloride, EIPA, benzamil, and phenamil (n = 36, 32, 30, and 28, respectively). Curves are fits with the logistic equation (see *Materials and Methods*). H, concentration-dependent curves for phenamil in the presence (▲, n = 32) or absence (△, same as in G) of TPeA (0.5 μM).

Results

Inhibition of TRPP3-Mediated $^{45}Ca^{2+}$ Uptake by Amiloride and Its Analogs. We first used radiotracer uptake assays to assess the whole-cell Ca^{2+} transport activities in *X. laevis* oocytes. Oocytes injected with TRPP3 mRNA exhibited increased Ca^{2+} entry, compared with the control (H_2O-injected) oocytes. In the presence of 500 μM amiloride, 100 μM EIPA, 10 μM benzamil, and 10 μM phenamil, $^{45}Ca^{2+}$ uptake decreased from 79 ± 9 to 46 ± 4 (58% remaining), 27 ± 4 (34%), 29 ± 5 (37%), and 38 ± 4 (48%) pmol/oocyte/30 min (n = 6, P = 0.008), respectively (Fig. 1B). These compounds had little effect on the Ca^{2+} transport of control oocytes, indicating that TRPP3-mediated Ca^{2+} transport was significantly inhibited by amiloride and its analogs.

Inhibition of TRPP3-Mediated Whole-Cell Currents by Amiloride Analogs. We next employed the two-microelectrode voltage clamp technique to examine the inhibitory effects of amiloride and its analogs. In TRPP3-expressing oocytes, large inward currents were evoked by adding 5 mM Ca^{2+} to the NaCl-containing solution at the holding potential of −50 mV. Currents were activated and reached a peak in 10~20 s after Ca^{2+} was added and then inactivated. The Ca^{2+}-activated TRPP3 inward current was reduced in the presence of extracellular amiloride at 100 μM (40.3 ± 8.6% inhibition, P = 0.0001, n = 18) or 500 μM (85.9 ± 11.3% inhibition, P = 0.0005, n = 20) (see, for example, Fig. 2A), but not at 10 μM (P = 0.2, n = 13), indicating a rather low-affinity inhibition. This inhibition by amiloride was reversible as the inward current recovered 8~10 min after washout (see representative tracing in Fig. 2A), which is also approximately the time required for evoking a second activation of the channel after the first activation (in the absence of amiloride) (Chen et al., 1999). Using a ramp voltage protocol, we showed that amiloride also exhibits its inhibitory effect at other membrane potentials, as shown by averaged current-voltage curves obtained in the presence and absence of amiloride (Fig. 2B).

Because amiloride is a low-affinity inhibitor of the TRPP3 channel, we wondered whether its analogs have similar effects on TRPP3. We tested the effects of EIPA, benzamil, and phenamil, which are formed by replacing one of the two amino groups in amiloride with more hydrophobic side chains (Fig. 1A). We found that EIPA, benzamil, and phenamil rapidly and reversibly block Ca^{2+}-activated TRPP3 channel activation at −50 mV as well as at other membrane potentials (Fig. 2, C–F). When currents obtained at −50 mV in the presence of various concentrations of amiloride and its analogs were averaged and fitted with the logistic equation (see *Materials and Methods*), we obtained the IC_{50} values of 143 ± 8 (n = 36), 10.5 ± 2.2 (n = 28), 1.1 ± 0.3 (n = 30), and 0.14 ± 0.04 μM (n = 25) for amiloride, EIPA, benzamil, and phenamil, respectively (Fig. 2G). Thus, the inhibition potency order is phenamil > benzamil > EIPA > amiloride, with the difference in affinity of roughly 10-fold between two consecutive inhibitors.

Our previous data showed that large TAA compounds, known as inhibitors of nonselective cation channels, inhibit TRPP3 (Dai et al., 2006). To gain insight into whether these inhibitors bind to the same site as amiloride analogs, we examined inhibition of phenamil in the presence of TPeA. We found that the IC_{50} value for phenamil is 4.30 ± 0.02 μM in the presence of 0.5 μM TPeA (the IC_{50} value for TPeA was 1.3 μM), which is 30-fold higher than the value in the absence of TPeA (Fig. 2H). These data suggest that the two classes of inhibitor compete for the same binding site in TRPP3.

In the absence of Ca^{2+}, the basal Na^+ current was also reversibly inhibited by 100 to 500 μM amiloride, 10 to 100 μM EIPA, 1 to 10 μM benzamil, and 0.03 to 1 μM phenamil,

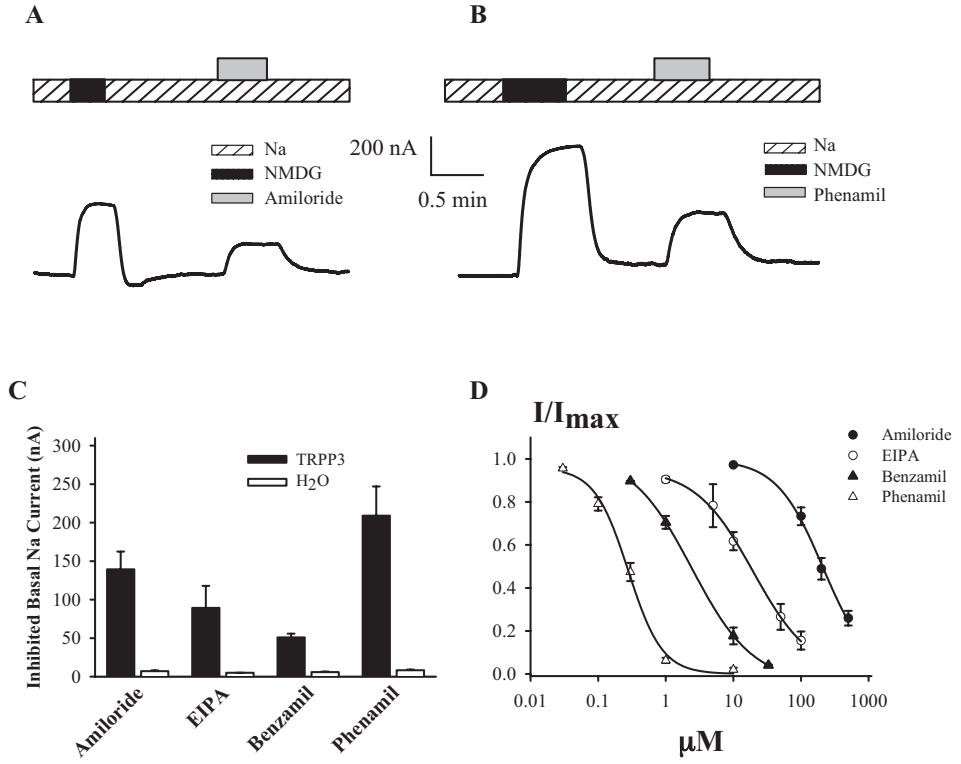

Fig. 3. Effects of amiloride analogs on the TRPP3-mediated basal Na^+ currents. A and B, representative current recording at −50 mV in an oocyte expressing TRPP3 in the presence or absence of amiloride (500 μM) (A) or phenamil (1 μM) (B). "NMDG" indicates the "Na" solution in which Na^+ was replaced by the equimolar *N*-methyl-D-glucamine. C, basal Na^+ currents at −50 mV inhibited by 500 μM amiloride, 100 μM EIPA, 10 μM benzamil, or 1 μM phenamil, in oocytes expressing TRPP3 or H_2O-injected oocytes. D, averaged concentration dependence of normalized basal Na^+ currents at −50 mV for various amiloride analogs. The IC_{50} values were estimated to be 155 ± 0.01 (n = 23), 12.2 ± 0.01 (n = 18), 2.43 ± 0.01 (n = 22), and 0.28 ± 0.04 μM (n = 22) for amiloride, EIPA, benzamil, and phenamil, respectively.

with similar affinity constants (Fig. 3) compared with the inhibition of Ca^{2+}-activated currents (Fig. 2G). With 500 μM amiloride, 100 μM EIPA, 10 μM benzamil, or 1 μM phenamil, the basal Na^+ currents of the TRPP3 channel were significantly and reversibly inhibited (Fig. 3, A–C). The basal Na^+ currents in H_2O-injected oocytes were not significantly inhib-

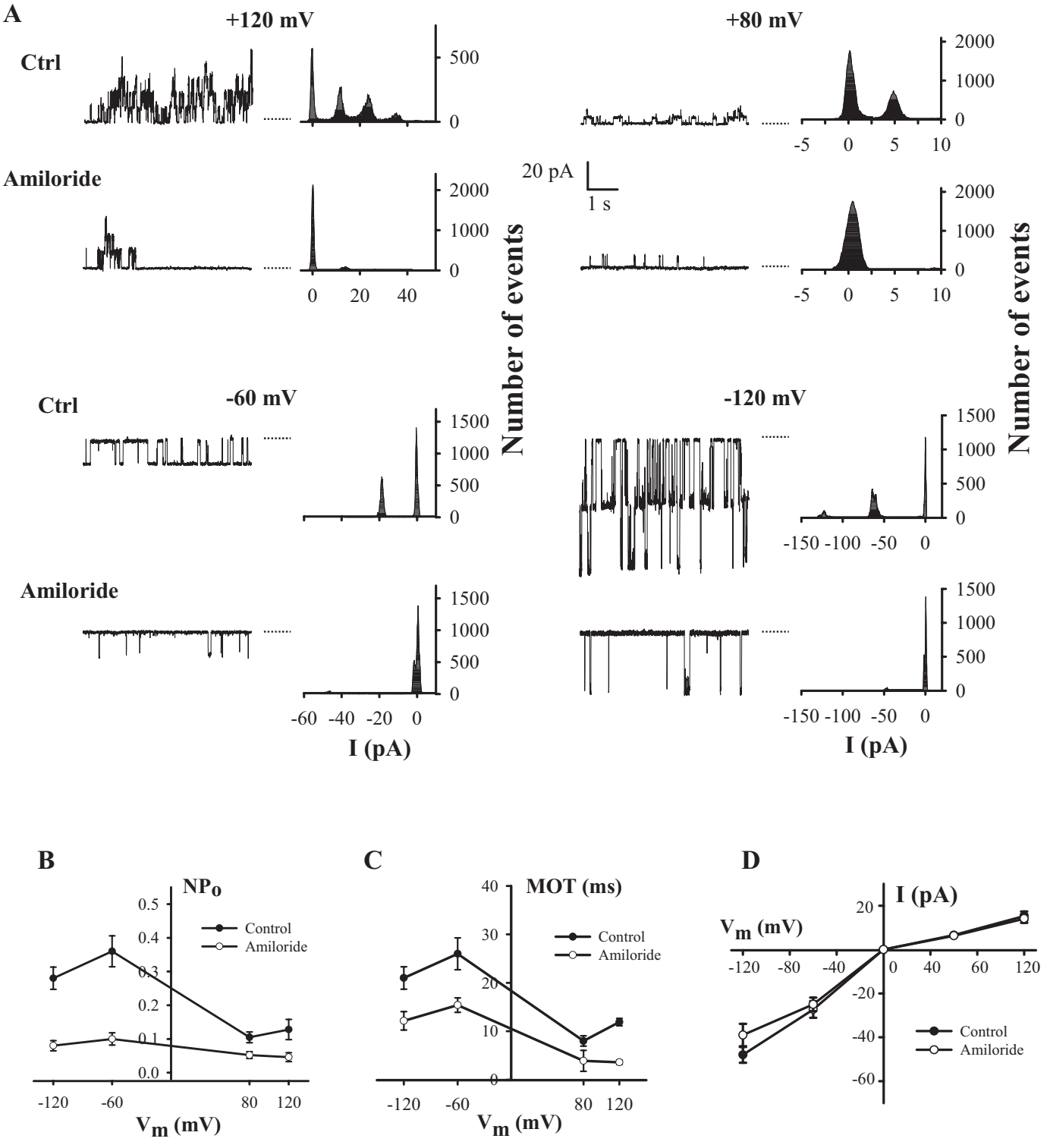

Fig. 4. Effects of amiloride on TRPP3 single-channel properties. The cell-attached mode of the patch clamp technique was used in these experiments. A, representative recordings (left) and the corresponding density plots (right) at indicated voltages in the presence pipette 123 mM K^+ (Control) ± 500 μM amiloride. The closed levels are indicated by horizontal dashed lines. Shown traces were Gaussian filtered at 200 Hz, using Clampfit 9. The tracings in the presence or absence of amiloride were from the same oocytes. B, averaged (n = 8) NP_o values at various V_m ± amiloride (500 μM). A two-way ANOVA analysis produced $P < 0.0001$ for amiloride and V_m, and $P = 0.008$ for the amiloride × V_m interaction. C, effects of amiloride on MOT. $P = 0.002$ for amiloride, $P < 0.0001$ for V_m, and $P = 0.01$ for the amiloride × V_m interaction. D, averaged single-channel amplitudes obtained in the presence or absence of amiloride (500 μM) (n = 15, $P > 0.05$).

ited by 500 μM amiloride or 1 μM phenamil (data not shown). The IC_{50} values were 209, 19.5, 2.4, and 0.28 μM for amiloride, EIPA, benzamil, and phenamil, respectively (Fig. 3D).

Inhibition of Single-Channel Activities of TRPP3 by Amiloride Analogs. To examine inhibitory effects of amiloride analogs on TRPP3 single-channel activities, we used the cell-attached mode of patch clamp. In the presence of 123 mM K^+ in the pipette, TRPP3 channel openings were observed in 245 of 296 patches in oocytes over-expressing TRPP3. With linear regression in negative ($-V_m$, $-20\sim-120$ mV) and positive membrane potentials ($+V_m$, $+20\sim+120$ mV), we calculated that TRPP3 has a larger inward single-channel conductance (399 $\pm$ 12 pS at $-V_m$, $n = 30$) than outward conductance (137 $\pm$ 10 pS at $+V_m$, $n = 26$), presumably because of inward rectification and the presence of asymmetrical concentrations of permeant ions on the two sides of the membrane (Liu et al., 2002). No channel openings of similar main conductance were observed in H_2O-injected control oocytes ($n = 20$).

We performed cell-attached recordings in the presence or absence of pipette amiloride from patches of the same oocyte to minimize variations as a result of changes in the surface expression of different oocytes. At both positive and negative voltages, amiloride (500 μM) significantly decreased TRPP3 single-channel NP_o but not the amplitude (Fig. 4). A two-way ANOVA analysis revealed that 500 μM amiloride significantly inhibited NP_o ($P < 0.0001$) and that NP_o value was voltage-dependent ($P < 0.0001$), with higher NP_o values at $-V_m$ (Fig. 4B). The MOT values were also altered by extracellular amiloride ($P = 0.002$) and were voltage-dependent ($P < 0.0001$), with higher MOT values at $-V_m$ (Fig. 4C). It is noteworthy that no effect on NP_o and MOT was observed when 10 μM amiloride was added to the pipette solution, indicative of low-affinity inhibition by amiloride. Likewise, we found that EIPA, benzamil, and phenamil, exhibit inhibitory effects on NP_o and MOT but not on the single-channel amplitude (Figs. 5–7). The inhibition by EIPA was concentration-dependent and the IC_{50} values for EIPA inhibition on NP_o were 13.7 $\pm$ 1.5 and 18.1 $\pm$ 0.8 μM at -120 and $+120$ mV, respectively ($P < 0.01$, $n = 20$) (Fig. 5B). The IC_{50} values on MOT were 25 $\pm$ 4 and 28 $\pm$ 5 μM, respectively ($P < 0.01$, $n = 20$) (Fig. 5C). Those for benzamil on NP_o were 0.5 $\pm$ 0.01 and 1.4 $\pm$ 0.3 μM at -120 and $+120$ mV ($P < 0.01$, $n = 11$), respectively, whereas those on MOT were 0.8 $\pm$ 0.03 and 1.7 $\pm$ 0.3 μM, respectively ($P < 0.01$, $n = 13$) (Fig. 6, B and C). Phenamil exhibited similar inhibition characteristics than its analogs but with higher potency. The IC_{50} values for phenamil on NP_o were 0.24 $\pm$ 0.04 and 0.39 $\pm$ 0.07 μM at -120 and $+120$ mV ($P < 0.05$, $n = 26$), respectively, whereas those on MOT were 0.45 $\pm$ 0.01 and 0.52 $\pm$ 0.08 μM, respectively ($P < 0.01$, $n = 19$) (Fig. 7, B and C). The inhibition effects on NP_o, MOT, and mean current by 500 μM amiloride,

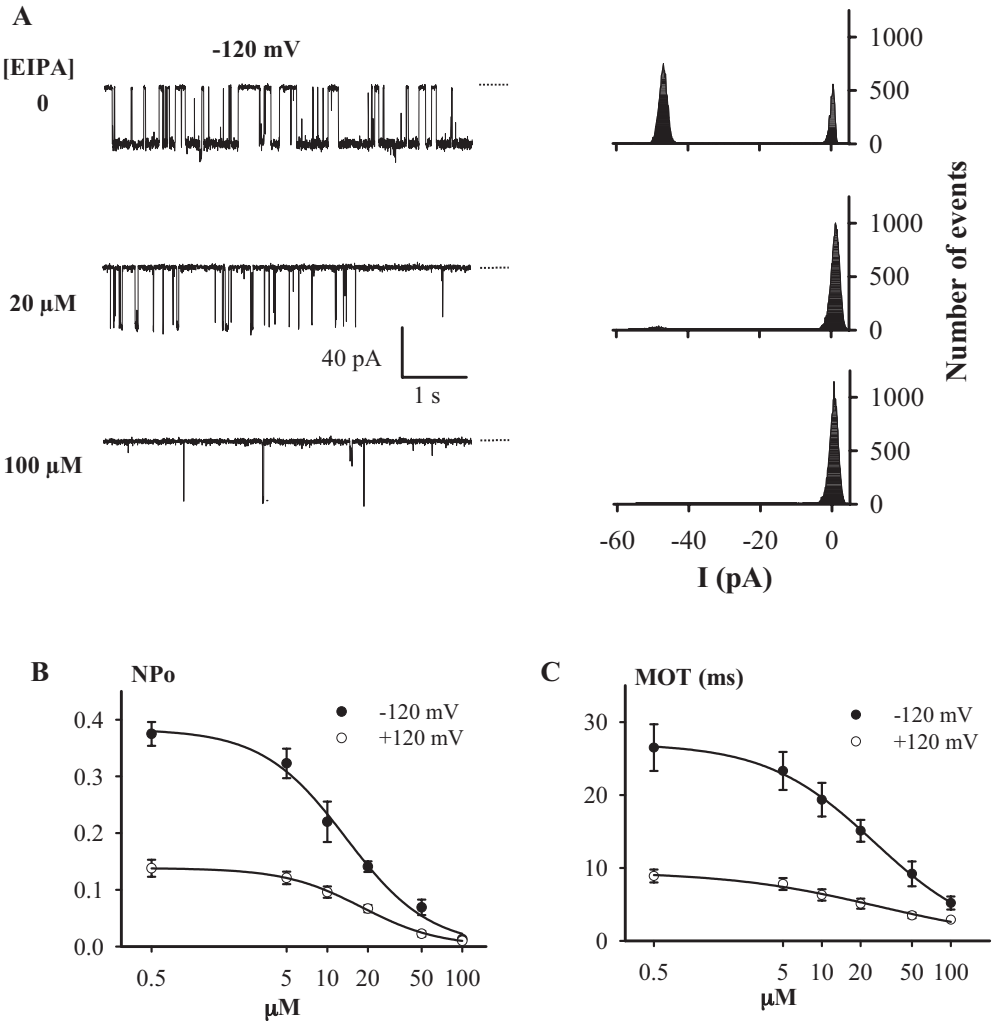

Fig. 5. Effects of EIPA. A, representative recordings (left) at -120 mV in the presence of 123 mM K^+ (control) in the pipette, plus 0, 0.5, 5, 10, 20, 50, or 100 μM EIPA, and the corresponding density plots (right). The tracings at different EIPA concentrations were from the same oocytes. B, concentration-dependent curves for the inhibition of NP_o by EIPA at -120 mV and $+120$ mV, respectively. Data were averaged from 20 determinations. The curves are fits by the Logistic equation. C, concentration-dependent curves for the inhibition of MOT by EIPA ($n = 20$).

100 μM EIPA, 1 μM benzamil, and 1 μM phenamil at $-V_m$ and $+V_m$ were compared (Fig. 8, A–C). It is noteworthy that we also examined the effects of intracellular amiloride analogs preinjected 3 h before experiments. No significant effect was observed (data not shown), suggesting that they do not exhibit similar inhibition from the intracellular side of the membrane.

Discussion

As a well known blocker of ENaC, Na^+/Ca^{2+} and Na^+/H^+ exchangers, nonselective cation channels, and voltage-gated K^+ and Ca^{2+} channels, amiloride also inhibits the responses to all taste stimuli (Gilbertson et al., 1993; Lilley et al., 2004), currents induced by the expression of polycystin-1 C-terminal fragments in *X. laevis* oocytes (Vandorpe et al., 2001), and those mediated by TRPP2 channels reconstituted in lipid bilayer or overexpressed in sympathetic neurons (González-Perrett et al., 2001; Delmas et al., 2004). It is noteworthy that recent reports showed that TRPP3 plays an important role in sour tasting and acid sensing (Huang et al., 2006; Ishimaru et al., 2006). TRPP3 is concentrated in the apical membrane (facing taste pores) of bipolar cells in taste buds, suggesting that it allows an initial cation influx triggered by low pH at the taste pore, which activates surrounding voltage-gated cation channels via local membrane depolarization and then leads to the firing of an action potential. In the entire length of the spinal cord, TRPP3 is present in neurons that project into the central canal, suggesting that it may also trigger an initial cation entry after a decrease in the canal pH (Huang et al., 2006). However, it remains unclear why TRPP3 responds to two very different pH ranges in the tongue and spinal cord. It is possible that polycystin-1L3 plays a role in acid sensing.

In the present study, we investigated the modulation of the TRPP3 channel function by amiloride and its analogs (phenamil, benzamil, and EIPA), using whole-cell and single-channel electrophysiology and radiotracer uptake measurements. These compounds inhibited both the Ca^{2+}-activated and basal TRPP3-mediated cation transports in *X. laevis* oocytes. In radiotracer uptake experiments, oocytes are not voltage-clamped (to negative membrane potentials, e.g., −50 mV), any significant Ca^{2+} entry will immediately lead to membrane depolarization, which slows down further Ca^{2+} entry. Thus, Ca^{2+} entry should not be sufficient in these experiments to induce TRPP3 channel activation and should reflect

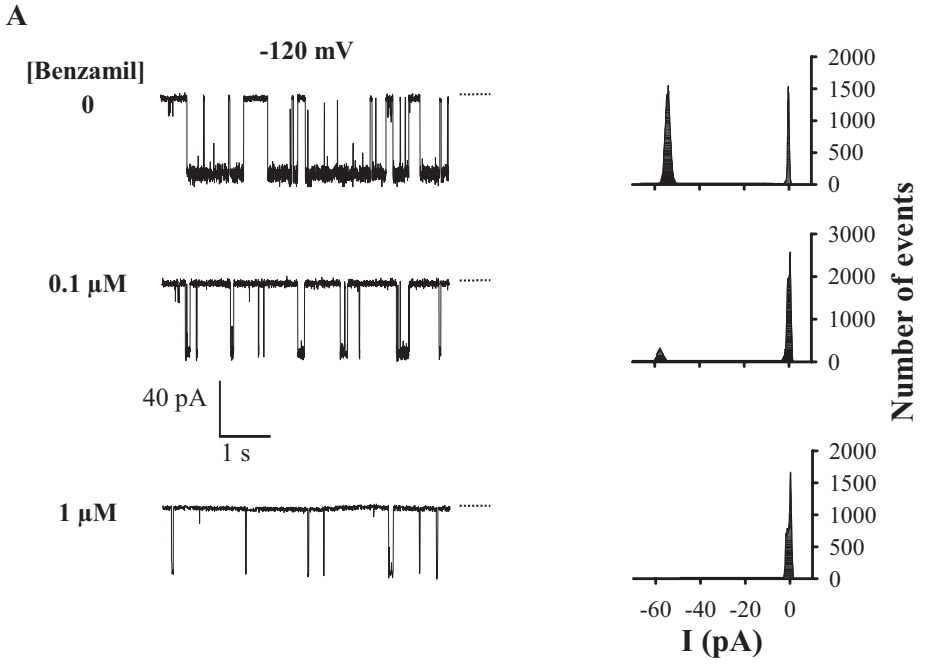

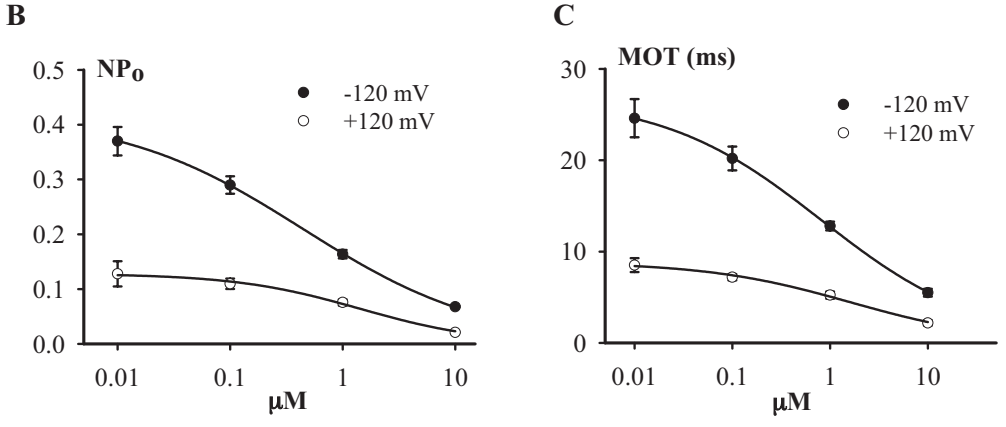

Fig. 6. Effects of benzamil. A, representative recordings (left) at −120 mV in the presence of benzamil at various concentrations and the corresponding density plots (right), from the same oocytes. B and C, concentration-dependent curves for the inhibition of NP_o (n = 24) and MOT (n = 20) by benzamil at −120 and +120 mV, respectively. Each point was averaged from 13 determinations.

the basal TRPP3 channel activity. In cell-attached experiments, because Ca^{2+} was absent in the pipette solution, single-channel activities correspond also to the basal TRPP3 function. In fact, so far we have been unable to conclude as to whether Ca^{2+} (5 mM) in the cell-attached pipette can induce activation of TRPP3 channels present in the patch. An important difference to the whole-cell voltage clamp may be that the Ca^{2+} entry through the tiny membrane patch under the pipette does not cause sufficient increase in the local intracellular Ca^{2+} concentration in the proximity of the patch to activate these few TRPP3 channels due to fast diffusion of Ca^{2+} ions.

Amiloride analogs are 2- to 3-fold more effective, as judged by IC_{50} values, in blocking the Ca^{2+}-activated current than the basal current. This might be due to the possibility that amiloride analogs are more potent inhibitors for the current carried by Ca^{2+} ions, which are approximately 5 times more permeant to TRPP3 than Na^+ (Chen et al., 1999). Another possibility is that the proportion of current already inhibited by 1 mM Mg in the solution differs between the basal and activation conditions. These inhibitors reduce the NP_o and MOT, but not the single-channel conductance. Because no rapid "flickery" block was observed, our data suggest that these inhibitors alter channel gating by binding to a site(s) on the channel protein outside the pore pathway, instead of competing with permeant ions such as Ca^{2+} and Na^+.

It is noteworthy that the hydrophobicity of the side chain, the molecular diameter, and the inhibition potency of these analogs follow the same order, phenamil > benzamil > EIPA > amiloride (Fig. 8D), which is different from that for ENaC (phenamil > benzamil > amiloride > EIPA) and Na^+/H^+ exchanger (phenamil > EIPA > amilorde, benzamil) (Kleyman and Cragoe, 1988), suggesting that these membrane proteins have different binding kinetics or structures for the inhibitors. The binding cassette in TRPP3 may have a hydrophobic environment that promotes binding of ligands of higher hydrophobicity or the size of the binding cassette may be closer to that of phenamil than the other inhibitors. We previously estimated that TRPP3 channel possesses a pore diameter of ~7 Å and a binding cassette of at least 13 Å for organic cation inhibitors (Dai et al., 2006). In that study, we found that the largest inhibitor TPeA, with a size of ~13 Å,

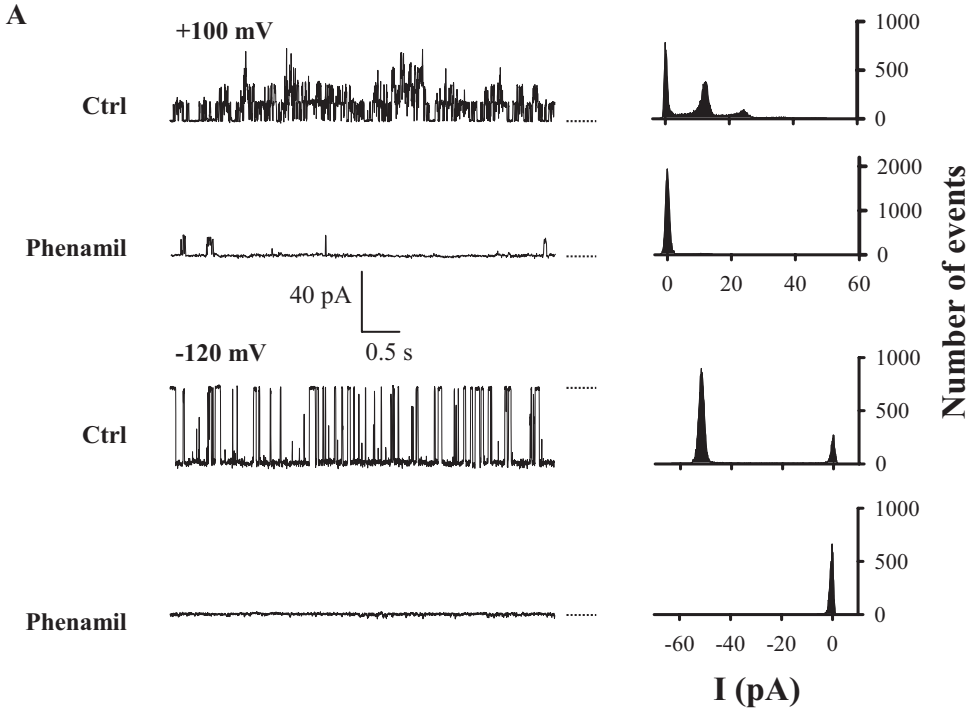

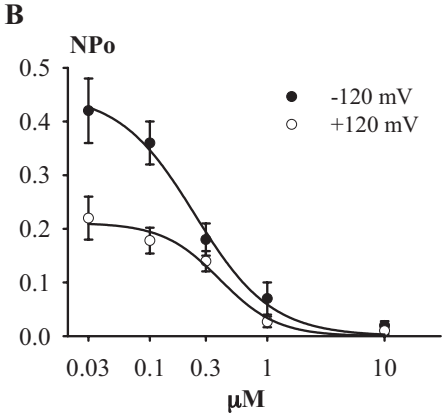

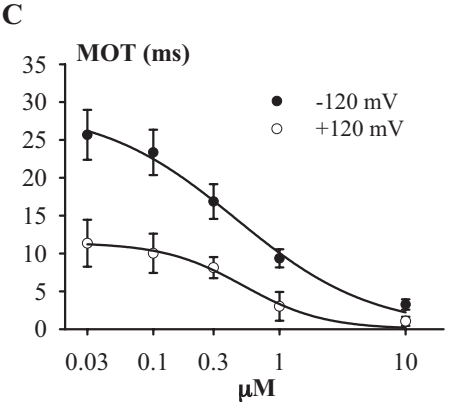

Fig. 7. Effects of phenamil. A, representative recordings (left) at +100 and −120 mV in the presence of phenamil at various concentrations and the corresponding density plots (right), from the same oocytes. B and C, concentration-dependent curves for the inhibition of NP_o (n = 26) and MOT (n = 19) by phenamil at −120 and +120 mV, respectively.

is the most potent of the organic cation inhibitors tested. We also found that these inhibitors, except tetrabutylammonium, reduce NP_o and MOT but not the single-channel conductance. This raises the possibility that amiloride analogs and organic cation inhibitors share the same binding site. This is supported by our finding that the IC_{50} value for phenamil augments by 30-fold in the presence of 0.5 μM TPeA.

Renal Na^+ reabsorption is crucial for Na^+ and body fluid homeostasis. Amiloride-sensitive Na^+ reabsorption constitutes a major ion transport pathway in the principal cells of cystic and noncystic collecting tubules (Hirsh, 2002). It has been reported that amiloride-sensitive nonselective channels with unclear molecular identities may contribute to Na^+ reabsorption in distal tubules, collecting ducts, cultured A6 kidney cells, hippocampus and Ehrlich-Lettre-ascites tumor cells (Chu et al., 2003; Lawonn et al., 2003). It is noteworthy that TRPP3 is present in the apical region of renal principal cells (Basora et al., 2002), and part of Na^+ reabsorption in collecting ducts was reported to be mediated by amiloride-sensitive nonselective cation channels (Vandorpe et al., 1997), suggesting that TRPP3 may contribute to renal Na^+ reabsorption. It is noteworthy that although TRPP3 channels overexpressed in *X. laevis* oocytes exhibit high unitary conductance and low sensitivity to amiloride inhibition, these parameters for in vivo TRPP3 channels in kidney and other organs might be substantially different because of possible presence of tissue-specific modulatory protein subunits. Thus, understanding effects of amiloride on the TRPP3 channel may help to determine its physiological roles in kidney and other tissues.

The mouse ortholog of TRPP3 is deleted in *krd* (kidney and retinal defects) mice (Keller et al., 1994; Nomura et al., 1998). TRPP3 may be one of the candidates linked to unmapped human genetic cystic disorders such as dominantly transmitted glomerulocystic kidney disease of postinfancy onset, isolated polycystic liver disease, and Hajdu-Cheney syndrome/serpentine fibula syndrome (Nomura et al., 1998). Although no evidence showed the direct involvement of TRPP3 in AD-PKD or ARPKD, a role for TRPP3 in cystogenesis is not excluded, as an interaction between TRPP3 and polycystin-1 exists (Murakami et al., 2005). Coexpression of TRPP3 together with polycystin-1 resulted in the expression of TRPP3 channels on the cell surface, whereas TRPP3 expressed alone was retained with the ER (Murakami et al., 2005). Monolayers formed by ARPKD principal cells of human fetal renal collecting ducts exhibit remarkably higher transepithelial Na^+ reabsorption than control monolayers (Rohatgi et al., 2003; Olteanu et al., 2006). It is noteworthy that this increased Na^+ movement is partially inhibited by amiloride with relatively low affinity. In contrast, the amiloride-sensitive Na^+ reabsorption is decreased in principal cells isolated from *bpk* ARPKD mice (Veizis et al., 2004). Because the protein mutated in these ARPKD cells does not resemble an ion channel or transporter, we speculate that it may regulate the surface membrane expression and/or function of yet-to-be-identified channels or transporters that are permeable to Na^+ with low sensitivity to amiloride. The regulation could be through physical binding or indirectly through a cascade pathway that links a PKD protein to an ion channel or transporter. It is noteworthy that a number of compounds, particularly amiloride and its analogs, can interfere with cyst growth in animal and in vitro studies (Ogborn, 1994).

In summary, TRPP3 may account for amiloride-sensitive

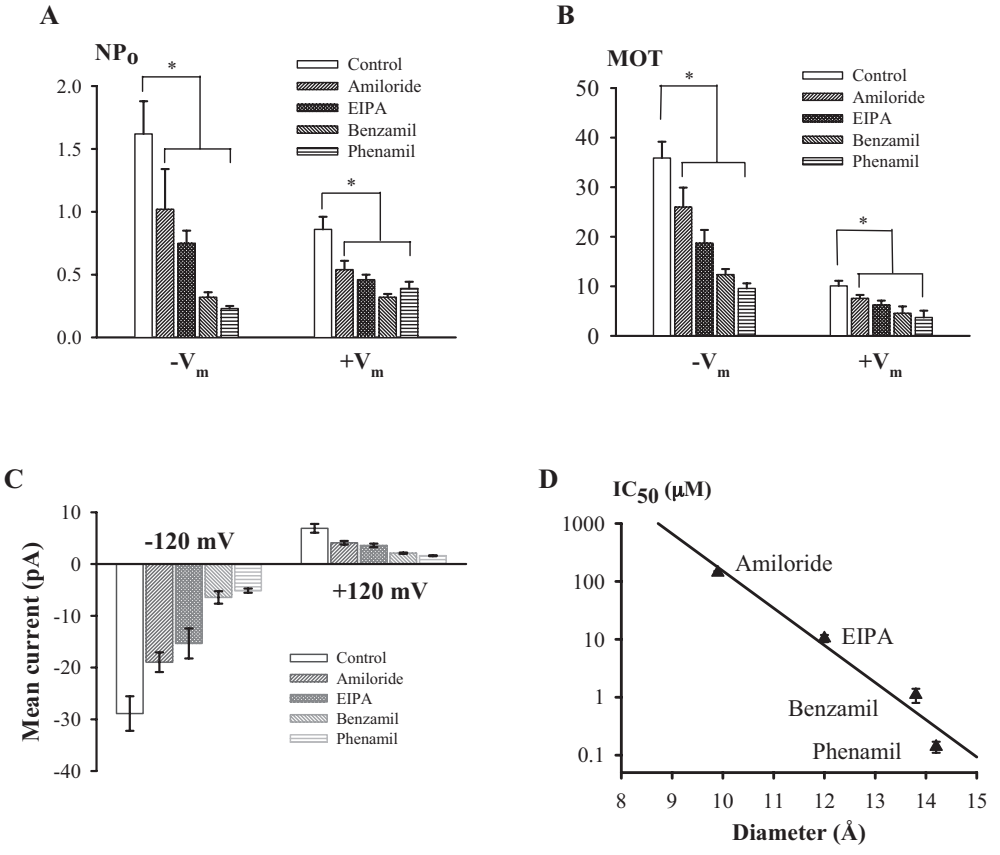

Fig. 8. Effects of amiloride analogs on TRPP3 single-channel parameters. Amiloride (500 μM), 100 μM EIPA, 1 μM benzamil, and 1 μM phenamil were used in the cell-attached experiments. A and B, inhibition of NP_o and MOT at $-V_m$ (n = 15–26) and $+V_m$ (n = 11–20). C, inhibition of mean currents at −120 mV (n = 15–26) and +120 mV (n = 11–20). D, IC_{50} values for amiloride and its analogs as a function of their molecular size. Ca^{2+}-activated whole-cell currents were used to determine the IC_{50} values averaged from 36, 25, 30, and 28 measurements for amiloride, EIPA, benzamil, and phenamil, respectively. The diameters of amiloride, EIPA, benzamil, and phenamil are 9.9, 12.0, 13.8, and 14.2 Å (unfolded model), respectively.

cation currents in some tissues and may play critical physiological roles in both neuronal and non-neuronal cells (e.g., in brain, retina and kidney) by mediating amiloride-sensitive, pH-dependent cation fluxes.

Acknowledgments

We thank Dr. Mariusz Klobukowski for help with the Spartan 4 program.

References

Basora N, Nomura H, Berger UV, Stayner C, Guo L, Shen X, and Zhou J (2002) Tissue and cellular localization of a novel polycystic kidney disease-like gene product, polycystin-L. *J Am Soc Nephrol* **13:**293–301.

Chen XZ, Vassilev PM, Basora N, Peng JB, Nomura H, Segal Y, Brown EM, Reeders ST, Hediger MA, and Zhou J (1999) Polycystin-L is a calcium-regulated cation channel permeable to calcium ions. *Nature* **401:**383–386.

Chu XP, Zhu XM, Wei WL, Li GH, Simon RP, MacDonald JF, and Xiong ZG (2003) Acidosis decreases low Ca^{2+}-induced neuronal excitation by inhibiting the activity of calcium-sensing cation channels in cultured mouse hippocampal neurons. *J Physiol* **550:**385–399.

Clapham DE (2003) TRP channels as cellular sensors. *Nature* **426:**517–524.

Dai XQ, Karpinski E, and Chen XZ (2006) Permeation and inhibition of polycystin-L channel by monovalent organic cations. *Biochim Biophys Acta* **1758:**197–205.

Delmas P, Nauli SM, Li X, Coste B, Osorio N, Crest M, Brown DA, and Zhou J (2004) Gating of the polycystin ion channel signaling complex in neurons and kidney cells. *FASEB J* **18:**740–742.

Doi Y and Marunaka Y (1995) Amiloride-sensitive and HCO3(-)-dependent ion transport activated by aldosterone and vasotocin in A6 cells. *Am J Physiol* **268:** C762–C770.

Gilbertson TA, Roper SD, and Kinnamon SC (1993) Proton currents through amiloride-sensitive Na^+ channels in isolated hamster taste cells: enhancement by vasopressin and cAMP. *Neuron* **10:**931–942.

González-Perrett S, Kim K, Ibarra C, Damiano AE, Zotta E, Batelli M, Harris PC, Reisin IL, Arnaout MA, and Cantiello HF (2001) Polycystin-2, the protein mutated in autosomal dominant polycystic kidney disease (ADPKD), is a Ca^{2+}-permeable nonselective cation channel. *Proc Natl Acad Sci U S A* **98:**1182–1187.

Hirsh AJ (2002) Altering airway surface liquid volume: inhalation therapy with amiloride and hyperosmotic agents. *Adv Drug Deliv Rev* **54:**1445–1462.

Huang AL, Chen X, Hoon MA, Chandrashekar J, Guo W, Trankner D, Ryba NJ, and Zuker CS (2006) The cells and logic for mammalian sour taste detection. *Nature* **442:**934–938.

Ishimaru Y, Inada H, Kubota M, Zhuang H, Tominaga M, and Matsunami H (2006) Transient receptor potential family members PKD1L3 and PKD2L1 form a candidate sour taste receptor. *Proc Natl Acad Sci U S A* **103:**12569–12574.

Keller SA, Jones JM, Boyle A, Barrow LL, Killen PD, Green DG, Kapousta NV, Hitchcock PF, Swank RT, and Meisler MH (1994) Kidney and retinal defects (Krd), a transgene-induced mutation with a deletion of mouse chromosome 19 that includes the Pax2 locus. *Genomics* **23:**309–320.

Kleyman TR and Cragoe EJ Jr. (1988) Amiloride and its analogs as tools in the study of ion transport. *J Membr Biol* **105:**1–21.

Kleyman TR and Cragoe EJ Jr (1990) Cation transport probes: the amiloride series. *Methods Enzymol* **191:**739–755.

Koulen P, Cai Y, Geng L, Maeda Y, Nishimura S, Witzgall R, Ehrlich BE, and Somlo S (2002) Polycystin-2 is an intracellular calcium release channel. *Nat Cell Biol* **4:**191–197.

Lawonn P, Hoffmann EK, Hougaard C, and Wehner F (2003) A cell shrinkage-induced non-selective cation conductance with a novel pharmacology in Ehrlich-Lettre-ascites tumour cells. *FEBS Lett* **539:**115–119.

Li Q, Liu Y, Shen PY, Dai XQ, Wang S, Smillie LB, Sandford R, and Chen XZ (2003) Troponin I binds polycystin-L and inhibits its calcium-induced channel activation. *Biochemistry* **42:**7618–7625.

Lilley S, LeTissier P, and Robbins J (2004) The discovery and characterization of a proton-gated sodium current in rat retinal ganglion cells. *J Neurosci* **24:**1013–1022.

Liu Y, Li Q, Tan M, Zhang YY, Karpinski E, Zhou J, and Chen XZ (2002) Modulation of the human polycystin-L channel by voltage and divalent cations. *FEBS Lett* **525:**71–76.

LopezJimenez ND, Cavenagh MM, Sainz E, Cruz-Ithier MA, Battey JF, and Sullivan SL (2006) Two members of the TRPP family of ion channels, Pkd1l3 and Pkd2l1, are co-expressed in a subset of taste receptor cells. *J Neurochem* **98:**68–77.

Murakami M, Ohba T, Xu F, Shida S, Satoh E, Ono K, Miyoshi I, Watanabe H, Ito H, and Iijima T (2005) Genomic organization and functional analysis of murine PKD2L1. *J Biol Chem* **280:**5626–5635.

Murata Y, Harada K, Nakajima F, Maruo J, and Morita T (1995) Non-selective effects of amiloride and its analogues on ion transport systems and their cytotoxicities in cardiac myocytes. *Jpn J Pharmacol* **68:**279–285.

Nauli SM, Alenghat FJ, Luo Y, Williams E, Vassilev P, Li X, Elia AE, Lu W, Brown EM, Quinn SJ, et al. (2003) Polycystins 1 and 2 mediate mechanosensation in the primary cilium of kidney cells. *Nat Genet* **33:**129–137.

Nomura H, Turco AE, Pei Y, Kalaydjieva L, Schiavello T, Weremowicz S, Ji W, Morton CC, Meisler M, Reeders ST, et al. (1998) Identification of PKDL, a novel polycystic kidney disease 2-like gene whose murine homologue is deleted in mice with kidney and retinal defects. *J Biol Chem* **273:**25967–25973.

Ogborn MR (1994) Polycystic kidney disease—a truly pediatric problem. *Pediatr Nephrol* **8:**762–767.

Olteanu D, Yoder BK, Liu W, Croyle MJ, Welty EA, Rosborough K, Wyss JM, Bell PD, Guay-Woodford LM, Bevensee MO, et al. (2006) Heightened epithelial Na^+ channel-mediated Na^+ absorption in a murine polycystic kidney disease model epithelium lacking apical monocilia. *Am J Physiol Cell Physiol* **290:**C952–C963.

Rohatgi R, Greenberg A, Burrow CR, Wilson PD, and Satlin LM (2003) Na^+ transport in autosomal recessive polycystic kidney disease (ARPKD) cyst lining epithelial cells. *J Am Soc Nephrol* **14:**827–836.

Sariban-Sohraby S and Benos DJ (1986) The amiloride-sensitive sodium channel. *Am J Physiol* **250:**C175–C190.

Stoner LC and Viggiano SC (2000) Apical nonspecific cation channels in everted collecting tubules of potassium-adapted ambystoma. *J Membr Biol* **177:**109–116.

Tytgat J, Vereecke J, and Carmeliet E (1990) Mechanism of cardiac T-type Ca^{2+} channel blockade by amiloride. *J Pharmacol Exp Ther* **254:**546–551.

Vandorpe DH, Chernova MN, Jiang L, Sellin LK, Wilhelm S, Stuart-Tilley AK, Walz G, and Alper SL (2001) The cytoplasmic C-terminal fragment of polycystin-1 regulates a Ca^{2+}-permeable cation channel. *J Biol Chem* **276:**4093–4101.

Vandorpe DH, Ciampolillo F, Green RB, and Stanton BA (1997) Cyclic nucleotide-gated cation channels mediate sodium absorption by IMCD (mIMCD-K2) cells. *Am J Physiol* **272:**C901–C910.

Veizis EI, Carlin CR, and Cotton CU (2004) Decreased amiloride-sensitive Na^+ absorption in collecting duct principal cells isolated from bpk ARPKD mice. *Am J Physiol Renal Physiol* **286:**F244–F254.

Wu G, Hayashi T, Park JH, Dixit M, Reynolds DM, Li L, Maeda Y, Cai Y, Coca-Prados M, and Somlo S (1998) Identification of PKD2L, a human PKD2-related gene: tissue-specific expression and mapping to chromosome 10q25. *Genomics* **54:**564–568.

Address correspondence to: Dr. Xing-Zhen Chen, 729 Medical Sciences Building, Department of Physiology, University of Alberta, Edmonton, Alberta, T6G 2H7, Canada. E-mail: xzchen@ualberta.ca